https://doi.org/10.5194/egusphere-2026-4704
Preprint. Discussion started: 24 August 2026

Amine Ozonation Products Promote Sulfate Formation and Accelerate New Particle Growth

Weina Zhang[1,2], Jiale Lao[1,2], Yao Zhou[1,2], Ruijing Li[1,2], Shangyu Zhu[1,2], Guiying Li[1,2], Yuemeng Ji[1,2], Taicheng An[1,2,*]

[1]Guangdong Key Laboratory of Environmental Catalysis and Health Risk Control, Guangdong-Hong Kong-Macao Joint Laboratory for Contaminants Exposure and Health, Institute of Environmental Health and Pollution Control, Guangdong University of Technology, Guangzhou, 510006, China.
[2]Guangdong Basic Research Center of Excellence for Ecological Security and Green Development, Key Laboratory for City Cluster Environmental Safety and Green Development of the Ministry of Education, School of Environmental Science and Engineering, Guangdong University of Technology, Guangzhou, 510006, China.

Correspondence to: Taicheng An (antc99@gdut.edu.cn)

Abstract. New particle formation (NPF) significantly influences aerosol burden and cloud condensation nuclei in the atmosphere, but whether amine ozonation products retain nucleation activity remains unclear. This study combines quantum chemical calculations and cluster dynamics simulations to investigate how OH-amine and CHO-amine promote sulfate formation and subsequent cluster growth. Both type amines are found to dominantly reduce SO_2 hydrolysis barrier in the presence of water clusters, and rate-limiting step is changes to ozonation step. Further analysis of growth pathways reveals NH_2OH and CH_2NOH exhibit flexible multi-core routes that accelerate progression toward critical sizes, whereas CH_3NHOH and CHO-amines are largely confined to single- or double-core pathways. Simulations of cluster formation rates show several ozonation products achieve rates comparable to their parent amines, indicating amine-driven NPF can persist after ozonation rather than terminating with the consumption of the parent species. Humidity strongly activates all systems, while temperature effects diverge sharply. OH-amine formation rates drop by 3 – 14 orders of magnitude from 280 to 320 K, whereas CHO-amines decrease by only about one order over the same range. Together, these results demonstrate that OH- and CHO-amines effectively accelerate sulfate-based NPF through favorable kinetics in humid environments.

Graphical abstract

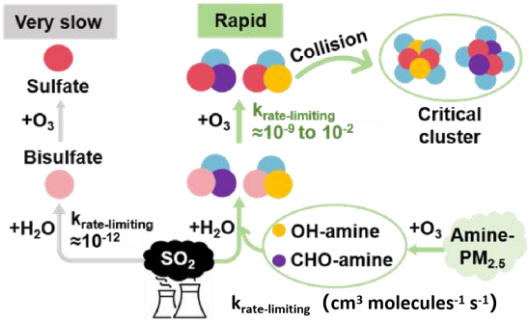

https://doi.org/10.5194/egusphere-2026-4704
Preprint. Discussion started: 24 August 2026

1 Introduction

New particle formation (NPF) is a major source of atmospheric particulate matter, exerting significant impacts on air quality, climate regulation, and human health. Sulfates, as one of the most abundant components of particulate matters (Brean et al., 2023; Li and Bourg, 2023), play a critical role in NPF (Brean et al., 2024; Deng et al., 2020). Amines have long been recognized as key contributors to sulfate formation, primarily through acid-base neutralization with sulfuric acid, in which amines themselves are converted into amine salts (Almeida et al., 2013; Yao et al., 2018). Recently, an additional pathway through which amines promote sulfate formation has been identified (Wang et al., 2020). Mechanistically, amines lower the energy barrier of the hydrolysis step of SO_2 from >30 kcal/mol to below the atmospheric feasibility threshold (~21 kcal/mol) (Wine et al., 1984; Lv et al., 2018; Liu et al., 2015), initiating the followed ozonation step (Wang et al., 2020). This pathway is especially favored during haze episodes, where humidity is high and ozone levels are elevated (Cai et al., 2024; Fang et al., 2019). By contrast, the conventional •OH-initiated SO_2 oxidation is thus suppressed (Brean et al., 2023; Brean et al., 2024) because •OH radical concentrations are low in dark condition during haze episodes.

However, the promotion effect of amines on sulfate formation is inherently limited because amines themselves are rapidly consumed by ozone. Upon ozonation, amines are converted into derivatives containing hydroxyl (-OH) or carbonyl (-CHO) groups, such as hydroxylamines, oximes, and amides (Ge et al., 2016; Zhang et al., 2025; Shen et al., 2021). For example, methylamine and dimethylamine, the most abundant atmospheric amines, ozonation yields products including NH_2OH, CH_2NOH, NH_2CHO, CH_3NHOH, and CH_3NHCHO (Ge et al., 2016; Zhang et al., 2025). These OH-/CHO-amines retain the amino group, and it is plausible that they possess chemical reactivity like their parent amines. Nevertheless, whether OH-/CHO-amines can sustain the promoting effect on sulfate formation remains entirely unknown.

To address this gap, we combine quantum chemical calculations and cluster dynamics simulations to investigate the five-representative amine ozonation products mentioned above, namely NH_2OH, CH_2NOH, NH_2CHO, CH_3NHOH, and CH_3NHCHO. We quantify their promotion effect on sulfate formation and evaluate their nucleation capability under broad temperature and humidity (RH = 20% – 100%, T = 280 – 320 K). Our results demonstrate that these amine ozonation products not only sustain but, in some cases, even enhance sulfate formation under typical winter haze conditions (RH >60%, T = 280 – 300 K). Our findings offer a scientific basis for improving atmospheric model predictions of sulfate formation in dark conditions during haze, which is required for evaluating the relevant impacts on air quality, climate regulation and human health.

2 Models and methods

2.1 Potential energy surface calculations

Quantum chemical calculations based on density functional theory (DFT) using Gaussian 09 (Vereecken and Francisco, 2012; Frisch et al., 2009; Li et al., 2017) are performed to elucidate the thermodynamic characteristics of SO_2 ozonation in the

https://doi.org/10.5194/egusphere-2026-4704
Preprint. Discussion started: 24 August 2026

presence of OH-/CHO-amines. All geometries of reactants, intermediates and products are optimized at the M06-2X/6-311G(d,p) level. To verify the connecting transition states, intrinsic reaction coordinate calculations are conducted. All single-point energies are refined using the higher-level M06-2X/6-311++G(3df,3pd) basis set (Fukui, 1981). Each stationary point along PES is confirmed by frequency calculations: all reactants, intermediates, and products exhibit no imaginary frequencies, whereas each transition state (TS) has exactly one. On the same PES, we define the energy barrier ($\Delta E^{\neq}$) as the single-point energy difference between the TS and reactants, and the reaction energy (ΔE_r) as the difference between the product (or intermediate) and reactants.

2.2 Kinetic rate constants

The reaction rate constants (k) are determined from the PES results using variational transition state theory (VTST) via the KiSThelP software (Canneaux et al., 2014; He and He, 2020). The sulfate formation is treated as a two-step process. The overall rate constant corresponds to the rate-limiting step, expressed as $k_{rate\text{-}limiting} = K_{eq}k$. Herein, K_{eq} is the equilibrium constant for the formation of the reactant complex, expressed as:

$$K_{eq}=exp(-\frac{\Delta E}{RT})$$

To account for the influence of atmospheric humidity on the promotion effect of target amines, we calculated the apparent pseudo-first order reaction rate constant (k_p). It is defined as:

$$k_p = k[H_2O]_n$$

Here, k is the reaction rate constant for the five amine types under different temperature and humidity conditions (Tables S1 – S3), and $[H_2O]_n$ denotes the concentration of water clusters (n = 1–3) under the corresponding humidity conditions (Anglada et al., 2013).

2.3 Hygroscopic growth pathway

The hygroscopic growth pathways of sulfate clusters containing OH-/CHO-amines are identified by calculating the energy reduction upon water addition. First, a global structural optimization of the sulfate clusters is performed using the artificial bee colony (ABC) algorithm (Zhang and Dolg, 2015; Bai et al., 2025). The ABCluster program is employed to automatically generate and pre-optimize 500 initial configurations with semi-empirical methods (Doye and Wales, 1998; Kirkpatrick et al., 1983; Stewart, 2007). From this set, the lowest-energy configuration is selected as the candidate structure and re-optimized at the M06-2X/6-311G(d,p) level. Its single-point energy is calculated using the higher-level M06-2X/6-311++G(3df,3pd) basis set. This procedure yields the globally energy-minimized configuration for a cluster at a specific water content. The pathway showing the steepest energy decrease is identified as the most favorable growth route.

As atmospheric humidity critically influences sulfate clusters (Loukonen et al., 2010; Ge et al., 2020), Their hydration distribution under different relative humidity (RH) conditions is analyzed to determine stable states. The relative abundance, x_n, of a hydrate containing n water molecules is given by (Henschel et al., 2016):

https://doi.org/10.5194/egusphere-2026-4704
Preprint. Discussion started: 24 August 2026

$$x_n = \left(\frac{p(H_2O)}{p^0}\right)^n x_0 e^{-\Delta E(n)/RT}$$

where $p(H_2O)$ is the partial pressure of water vapor, p^0 is the reference pressure (1 atm), n is the number of water molecules, ΔE is the energy change during cluster formation, R is the universal gas constant, T is the temperature, and x_0 is the fraction of the dry cluster under the normalization condition $\sum_0^4 x_n = 1$.

2.4 ACDC simulation

The Atmospheric Cluster Dynamics Code (ACDC) (Mcgrath et al., 2012; Liu et al., 2022) is used to simulate the collision-evaporation balance, formation rates, and growth pathways of the sulfate clusters. The simulated system comprises clusters of the form (OH-/CHO-amine)$_m(H_2O)_n$, with m ranging from 0 to 3 and n from 0 to 4. In these simulations, the concentration of OH-/CHO-amine is fixed at 1 ppt, while the water concentration ([H_2O]) is varied from 10^{15} to 10^{17} molecules cm^{-3} to assess its influence on nucleation. The primary simulations are run at 300 K, with additional sets at 280 K and 320 K to evaluate temperature effects. ACDC calculates the steady-state cluster formation rate and identifies dominant growth pathways by birth-death equation:

$$\frac{dC_i}{dt} = \frac{1}{2}\sum_{j<i} \beta_{j,(i+j)} C_j C_{i-j} + \sum_j \gamma_{(i+j)\to i} C_{(i+j)} - \sum_j \beta_{i,j} C_i C_j - \frac{1}{2}\sum_{j<i} \gamma_{i\to j} C_i + Q_i - S_i$$

where i denotes a cluster whose concentration is given by this equation, j is another cluster in the system, C_i is the number density of cluster i, $\beta_{i,j}$ is the collision coefficient between clusters i and j, and $\gamma_{i\to j}$ is the evaporation coefficient for the fragmentation of a cluster i into two smaller clusters (one of which is j). The ratio of the cluster collision coefficient β_i to the evaporation rate $\gamma_{(i+j)\to i}$ is denoted by R, which is expressed as $\beta_{cluster} C_{water}/\sum\gamma$. Q_i represents the external source term for i, and S_i includes other possible sink mechanisms for cluster i.

3 Results and discussion

3.1 Reaction kinetics of sulfate formation catalyzed by OH-/CHO-amine

Previous reports have established that sulfate formation proceeds via SO_2 hydrolysis and ozonation in sequence, with SO_2 hydrolysis identified as the rate-limiting step (Wang et al., 2020). Consistent with this framework, our PES results show that both OH- and CHO-substituted amines effectively promote sulfate formation by lowering the energy barrier for the SO_2 hydrolysis step when assisted by water clusters (Fig. S1 – S9 for OH-amines and Fig. S10 – S18 for CHO-amines). Taking the single-water system as an example, CH_3NHOH, NH_2OH, and CH_2NOH lower the hydrolysis barrier from the uncatalyzed value of 33.11 kcal/mol to 2.57, 5.36, and 19.42 kcal/mol, respectively (Fig. 1a), thereby rendering this step kinetically accessible. Interestingly, however, while OH-amines are highly effective in catalyzing hydrolysis, they do not similarly reduce the barrier for the subsequent ozonation step (Fig. 1b). As a result, the presence of OH-amines shifts the rate-limiting step from the high-barrier hydrolysis (33.11 kcal/mol) to the ozonation stage, which now features a considerably lower barrier of 17.20

https://doi.org/10.5194/egusphere-2026-4704
Preprint. Discussion started: 24 August 2026

– 24.25 kcal/mol. Beyond the single-water case, this promotional efficiency is further amplified by larger water clusters. For instance, the barrier of the SO_2 hydrolysis step decreases from positive values (as seen with a single H_2O) to negative values when $(H_2O)_3$ clusters participate in the reaction (Fig. 1c), indicating that the hydrolysis can become nearly barrierless under such conditions. As a net result, the overall effective barrier for the coupled hydrolysis–ozonation process drops to 17.27 – 17.86 kcal/mol (Fig. 1d and 1e), since the preceding hydrolysis is no longer rate-limiting. Given that atmospheric concentrations of $(H_2O)_2$ and $(H_2O)_3$ clusters increase with relative humidity (Anglada et al., 2013; Xiong et al., 2025), the OH-amine-mediated SO_2 hydrolysis pathway becomes particularly efficient under humid conditions, thus strongly favoring sulfate formation.

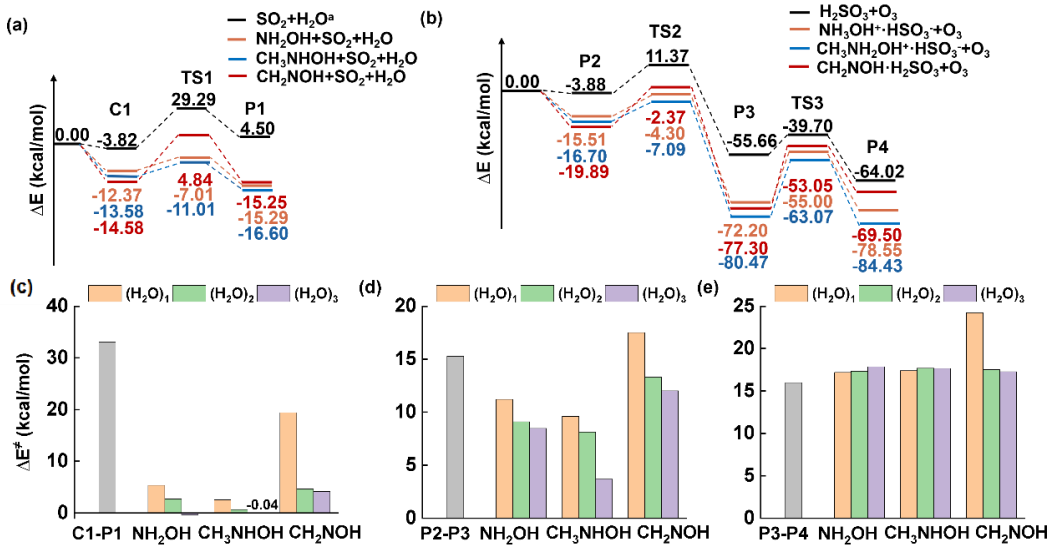

Figure 1 PESs and energy barriers for sulfate formation mediated by OH-amines. PES for (a) the SO_2 hydrolysis reaction and (b) the subsequent ozonation reaction in the presence of an OH-amine alone. Variation of the energy barrier ($\Delta E^{\neq}$) in (c) hydrolysis (step C1→P1), and (d-e) ozonation (step P2→P3 and P3→P4) with $(H_2O)_n$. [a]Value from Liu, et al. J. Phys. Chem. A 2015.

In comparison with OH-amines, CHO-substituted amines also exhibit a catalytic effect on sulfate formation, but their promotion effect is considerably more limited. For example, in the single-water system, NH_2CHO and CH_3NHCHO reduce the hydrolysis barrier from 33.11 kcal/mol to 29.09 and 22.30 kcal/mol, respectively, the values that are noticeably higher than those of OH-amines (which range from 2.57 to 19.42 kcal/mol, Fig. 2a). These reduced barriers remain above the commonly accepted threshold of ~21 kcal/mol for kinetically efficient gas-phase processes under ambient conditions, indicating that the hydrolysis step is still too slow to proceed effectively in the atmosphere. Furthermore, unlike the case of OH-amines (where the rate-limiting step shifts to ozonation with barriers of 17 – 24 kcal/mol), CHO-amines do not lower the ozonation barrier at all under single-water conditions (Fig. 2b). The ozonation step therefore remains highly unfavorable, and the overall reaction is still hindered by both high barriers. However, when larger water clusters, particularly $(H_2O)_3$, participate in the reaction, the situation changes dramatically. The hydrolysis barrier drops markedly to 11.51 and 9.51 kcal/mol for NH_2CHO and CH_3NHCHO, respectively (Fig. 2c). Concurrently, the overall barrier of the rate-determining step is defined by the ozonation

https://doi.org/10.5194/egusphere-2026-4704
Preprint. Discussion started: 24 August 2026

or the combined process, and falls to 16.6 and 9.9 kcal/mol (Fig. 2d and 2e) that are well below the kinetic threshold. Consequently, with the assistance of $(H_2O)_3$, the CHO-amine-mediated pathway becomes kinetically feasible under atmospheric conditions, despite its inferiority to the OH-amine routes. This finding reveals that high-humidity environments, in which $(H_2O)_3$ clusters are sufficiently abundant, are an essential prerequisite for initiating sulfate formation through CHO-amine pathway, because only under such conditions the hydrolysis barrier be lowered enough to allow the subsequent steps to proceed at appreciable rates.

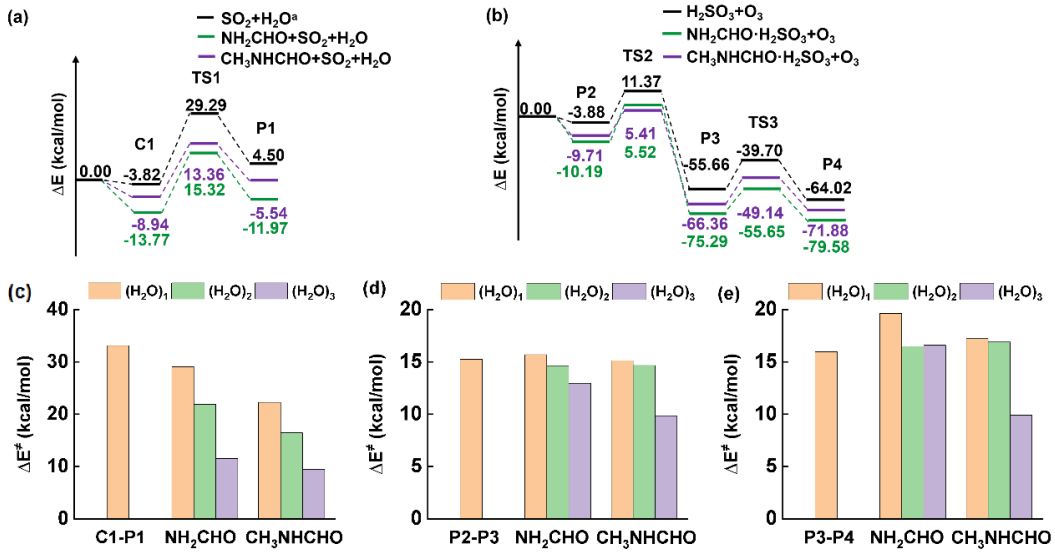

Figure 2 PESs and energy barriers for sulfate formation mediated by CHO-amines. PES for (a) the SO_2 hydrolysis reaction and (b) the subsequent ozonation reaction in the presence of an OH-amine alone. Variation of the energy barrier ($\Delta E^{\neq}$) in (c) hydrolysis (step C1→P1), and (d-e) ozonation (step P2→P3 and P3→P4) with $(H_2O)_n$. [a]Value from Liu, et al. J. Phys. Chem. A 2015.

Beyond the above PES analysis, the kinetic behavior of the SO_2 hydrolysis step directly determines its competitiveness against other SO_2 transformation pathways in the atmosphere. To quantitatively assess this competition, the effects of temperature (T) and relative humidity (RH) on the apparent pseudo-first-order rate constant (k_p) were evaluated for the hydrolysis step in both amine systems. Specifically, k_p was computed from the intrinsic hydrolysis rate constants (Tables S1 – S3) combined with the equilibrium concentrations of water monomers, dimers, and trimers ([H_2O], [$(H_2O)_2$], [$(H_2O)_3$]) at each specified RH and T, because the hydrolysis proceeds through parallel channels involving different water clusters. The computed k_p values, increase markedly with both rising T and RH for each amine specie (Fig. 3), revealing a positive synergistic effect. This synergy arises because higher T accelerates the intrinsic reaction rates, while higher RH also increases the populations of larger water clusters (especially dimers and trimers), which are more effective in lowering the hydrolysis barrier as already demonstrated in Fig. 1 and 2. Taking the OH-amine system as an example (Fig. 3a), for NH_2OH, raising T from 280 K to 320 K at a fixed RH of 60% increases k_p from 3.64×10^{24} to 9.62×10^{25} s^{-1}, with a nearly 26-fold enhancement. Similarly, at a constant T of 300 K, an increase in RH from 20% to 100% elevates k_p from 7.09×10^{24} to 3.61×10^{25} s^{-1}. That means CH_3NHOH exhibits a comparable trend, with k_p values ($10^{24} – 10^{26}$ s^{-1}) remaining consistently high across a wide range

https://doi.org/10.5194/egusphere-2026-4704
Preprint. Discussion started: 24 August 2026

of conditions, indicating that OH-amine-mediated hydrolysis is kinetically robust even under moderate temperature and humidity.

In contrast, the CHO-amine pathway is less efficient, with k_p values typically 3 – 6 orders of magnitude lower than those of OH-amines under equivalent conditions (Fig. 3b). Nevertheless, this pathway exhibits a striking sensitivity to humidity, which is crucial for its activation. For instance, for CH_3NHCHO, increasing T from 280 to 320 K at RH = 60% raises k_p from 2.50×10^{16} to 1.21×10^{19} s^{-1}, a gain of nearly three orders of magnitude. Even more notably, at 300 K, elevating RH from 20% to 100% boosts k_p by more than two orders of magnitude, reaching 3.31×10^{18} s^{-1}. This dramatic RH-dependence explains that the CHO-amine pathway relies almost entirely on the participation of $(H_2O)_3$ clusters to overcome the hydrolysis barrier (Fig. 2c). Consequently, the CHO-amine route is only viable under high-humidity conditions (e.g., RH > 80%), where the abundance of larger water clusters is sufficient to drive the reaction. Under such circumstances, it can serve as a supplemental, albeit secondary, source of sulfate, contributing to NPF in moist atmospheric environments.

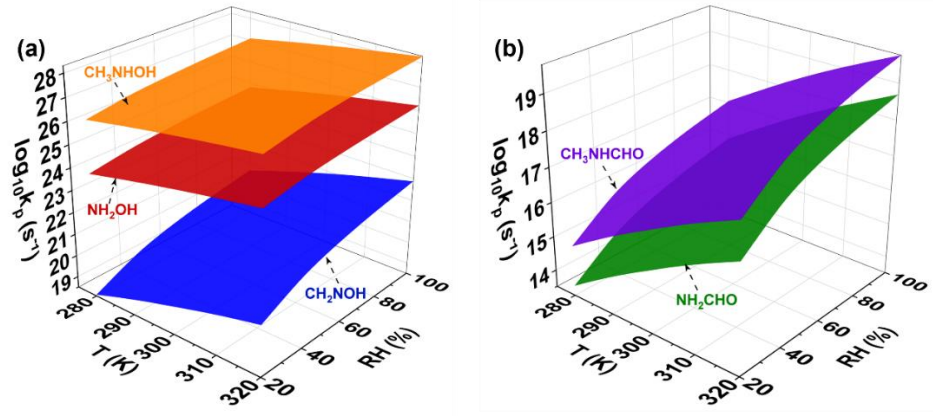

Figure 3 Effects of atmospheric temperature and humidity on k_p for the SO_2 hydrolysis reaction in (a) OH-amine and (b) CHO-amine systems.

In summary, regardless of whether they are OH- or CHO-substituted, their k_p values (ranging from 10^{24} to 10^{26} s^{-1} for OH-amines and from 10^{16} to 10^{19} s^{-1} for CHO-amines) indicate that the hydrolysis pathway has the kinetic capacity to compete with the •OH-initiated oxidation route, which has a reported k_p of 1.3×10^6 s^{-1}, under ambient conditions (Long et al., 2017). This comparison suggests that even the less efficient CHO-amine pathway can compete with the conventional oxidation channel in terms of reaction rate under favorable humidity conditions. More importantly, the catalytic efficiency of these amine derivatives with that of their parent amine, dimethylamine (DMA), were further compared. A previous study reported a rate constant of 4.53×10^{-9} molecules^{-1} cm^3 s^{-1} for the DMA–$(H_2O)_2$-mediated SO_2 hydrolysis at 300 K and RH = 100% (Wang et al., 2020). Under identical conditions (300 K, RH = 100%), the corresponding rate constants for the ozonation products of DMA, namely CH_3NHOH and CH_3NHCHO, reach 2.34×10^{11} and 2.04 molecules^{-1} cm^3 s^{-1}, respectively (Fig. S19–S20), that are approximately 20 and 9 orders of magnitude higher than that of the parent DMA. This dramatic enhancement indicates that the oxidation products of DMA retain, and in fact vastly exceed, the parent amine's ability to catalyze sulfate formation.

https://doi.org/10.5194/egusphere-2026-4704
Preprint. Discussion started: 24 August 2026

3.2 Hygroscopic growth of clusters containing OH-/CHO-amine–sulfate complexes

To further evaluate the nucleation potential of the amines investigated above, we simulated the hygroscopic growth of clusters containing an OH-/CHO-amine–sulfate complex as the core, tracking their structural evolution, diameter, and binding energy as a function of added Core or H_2O units (Table 1). For clusters containing NH_2OH or CH_2NOH, the critical diameter of ~1.1 nm is reached upon forming the $(Core)_3 \cdot (H_2O)_4$ structure. As more Core or H_2O units are added, the binding energy decreases markedly; this progressive decline in binding energy indicates that the growth process is thermodynamically spontaneous. Taking the NH_2OH system as an example, the binding energy at the critical size ($(Core)_3 \cdot (H_2O)_4$) reaches -106.48 kcal/mol, relative to a reference state of a single Core. In the CH_3NHOH-containing system, a similar critical diameter (~1.04 nm) is attained at the $(Core)_2 \cdot (H_2O)_4$ configuration with one fewer Core unit than required in the NH_2OH system. This reduced core requirement can be attributed to the larger molecular size of CH_3NHOH compared to NH_2OH, which enables the cluster to reach the critical dimension more efficiently with fewer core species. For the CHO-amine systems (NH_2CHO and CH_3NHCHO), the critical diameter (1.02 – 1.11 nm) is also achieved in the $(Core)_2 \cdot (H_2O)_4$ configuration. Their corresponding binding energies at this critical size are -76.15 and -74.23 kcal/mol, respectively, that are substantially more negative than those of their respective single-core, indicating that the multi-core clusters are more thermodynamically stable. Collectively, these results demonstrate that both OH- and CHO-substituted amines can serve as stable nucleation, guiding sulfate-containing clusters to the critical size through sequential uptake of water molecules or additional core species. This thermodynamic favourability, combined with the kinetic competitiveness established in the preceding sections, underscores the potential importance of these amine derivatives in atmospheric NPF.

Table 1 Variations in diameter (D) and binding energy (ΔE) for the five sulfate–amine clusters across the simulated size range.

	NH_2OH		CH_3NHOH		CH_2NOH		NH_2CHO		CH_3NHCHO	
	D (Å)	ΔE (kcal/mol)	D (Å)	ΔE (kcal/mol)	D (Å)	ΔE (kcal/mol)	D (Å)	ΔE (kcal/mol)	D (Å)	ΔE (kcal/mol)
Core	5.68	0.00	6.28	0.00	6.87	0.00	6.00	0.00	6.85	0.00
$Core \cdot H_2O$	6.13	-12.56	7.11	-12.55	7.27	-11.34	6.31	-13.95	6.81	-14.91
$Core \cdot (H_2O)_2$	6.31	-25.04	7.44	-22.75	7.53	-13.86	6.88	-27.12	7.32	-26.01
$Core \cdot (H_2O)_3$	6.92	-34.81	7.78	-29.62	8.00	-29.57	7.20	-38.44	7.73	-33.66
$Core \cdot (H_2O)_4$	7.62	-42.73	8.22	-40.01	8.15	-33.76	7.62	-43.44	8.28	-45.06
$(Core)_2$	8.19	-42.03	8.24	-35.31	7.90	-15.73	8.28	-33.80	8.74	-43.87
$(Core)_2 \cdot H_2O$	8.48	-48.97	8.67	-39.80	8.14	-23.99	8.65	-45.07	8.96	-51.32
$(Core)_2 \cdot (H_2O)_2$	8.57	-63.14	9.35	-54.39	8.31	-36.51	8.89	-59.65	9.75	-59.51
$(Core)_2 \cdot (H_2O)_3$	8.74	-68.63	9.94	-59.08	8.52	-45.85	9.41	-69.01	10.09	-66.88
$(Core)_2 \cdot (H_2O)_4$	8.94	-76.17	10.39	-71.28	8.73	-56.32	10.20	-76.15	11.09	-74.23
$(Core)_3$	9.57	-65.51			9.40	-37.30				
$(Core)_3 \cdot (H_2O)_1$	9.84	-72.47			9.70	-49.09				
$(Core)_3 \cdot (H_2O)_2$	10.40	-89.88			10.47	-57.50				
$(Core)_3 \cdot (H_2O)_3$	10.74	-96.89			10.96	-79.01				
$(Core)_3 \cdot (H_2O)_4$	11.01	-106.48			11.27	-84.29				

https://doi.org/10.5194/egusphere-2026-4704
Preprint. Discussion started: 24 August 2026

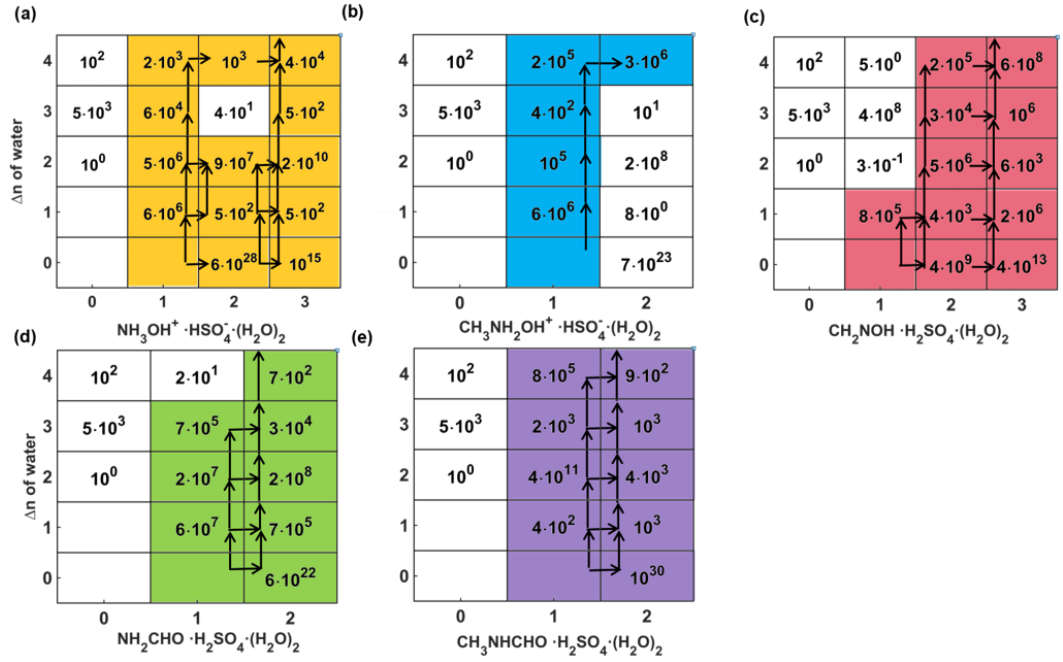

Figure 4 Collision-to-evaporation coefficient (R) along the growth pathways of sulfate clusters containing OH-/CHO-amines at 300 K and $[H_2O] = 10^{17}$ molecules cm^{-3}. (a–c) OH-amine systems: NH_2OH, CH_3NHOH, and CH_2NOH. (d–e) CHO-amine systems: NH_2CHO and CH_3NHCHO.

To systematically identify the dominant growth pathways under atmospheric conditions, we first calculate the collision coefficient (R) between a cluster (Core)m·(H_2O)n and a single Core or H_2O molecule at 300 K and $[H_2O] \approx 10^{17}$ molecules cm^{-3}. We adopt $R > 10^2$ as a criterion for feasible growth steps, because such a high collision frequency ensures that the addition event occurs rapidly enough to compete with other loss processes (e.g., evaporation or coagulation) under typical tropospheric conditions. The resulting pathway networks (Fig. 4) then reveal significant differences among amine derivatives. For the OH-amines (NH_2OH and CH_2NOH), they exhibit flexible single-, double-, and triple-core cooperative pathways (Fig. 4a and c) through multiple parallel routes. In stark contrast, CH_3NHOH, although also an OH-amine, follows exclusively a single-core addition route (Fig. 4b), revealing that even within the same functional class, the methyl substitution severely restricts the accessible pathways. For the CHO-amines (NH_2CHO, CH_3NHCHO), the networks are largely confined to single- and double-core routes (Fig. 4d and e) with no evidence of triple-core cooperation. This restriction implies that their growth is less adaptable to varying environmental conditions or cluster compositions. Overall, the broader growth flexibility observed for the OH-amines (except CH_3NHOH) underscores their potentially greater importance in facilitating the later stages of atmospheric particle formation. Specifically, the availability of multi-core pathways enables clusters to increase in size and mass more efficiently through simultaneous addition of multiple core species, which may accelerate the transition from clusters to critical sizes, which is a key step in NPF. In contrast, the limited route diversity of CHO-amines likely hinders their ability to sustain rapid growth, making them less influential in NPF.

https://doi.org/10.5194/egusphere-2026-4704
Preprint. Discussion started: 24 August 2026

3.3 Humidity-driven formation rates of critical clusters

Building on the growth pathway networks identified above, we employed the Atmospheric Cluster Dynamics Code (ACDC) model to simulate how temperature and humidity control the formation rate (J) of critical clusters containing OH-/CHO-amines. Since humidity has been established as the dominant factor promoting sulfate formation in the preceding sections, we first investigated its role in the subsequent critical cluster formation.

At 300 K, the formation rate J for all amine systems increases strongly with atmospheric water concentration ([H_2O]) (Fig. 5), consistent with the humidity-enhanced hydrolysis kinetics demonstrated earlier. Specifically, when [H_2O] increases from 10^{15} to 10^{17} molecules cm^{-3}, J rises by 3 – 6 orders of magnitude for critical clusters containing OH-amines (NH_2OH, CH_3NHOH, CH_2NOH) (Fig. 5a), and by approximately 3 orders of magnitude for those containing CHO-amines (NH_2CHO, CH_3NHCHO) (Fig. 5b). This pronounced humidity dependence reflects the combined effect of increased water cluster concentrations, which facilitate both hydrolysis and subsequent cluster growth, and the enhanced collision frequencies under humid conditions.

A key finding emerging from these simulations is the functional equivalence between certain amine oxidation products and their parent amines. For instance, over the same humidity range, the J values for clusters containing CH_2NOH and NH_2CHO (10^{11}–10^{14} cm^{-3} s^{-1}) (Fig. 5a) are of the same order of magnitude as those for clusters containing the parent methylamine (CH_3NH_2) (Fig. 5c), despite their distinct functional groups and reaction pathways. Similarly, under high humidity ([H_2O] = 10^{17} molecules cm^{-3}), the J value for CH_3NHCHO reaches 5.00×10^{13} cm^{-3} s^{-1} (Fig. 5a), which is comparable to that of the parent DMA system (~10^{13} cm^{-3} s^{-1}) (Fig. 5c). This functional equivalence demonstrates that OH- and CHO- amines can sustain cluster formation capacities comparable to their parent amines. Consequently, even as atmospheric amines undergo oxidative aging, their degradation products retain the ability to drive continuous NPF under humid conditions, thereby extending the effective lifetime of amine-mediated nucleation in the atmosphere.

In contrast to the positive effect of humidity, elevated temperature exerts a suppressive effect on cluster formation. At a fixed water concentration of [H_2O] = 10^{17} molecules cm^{-3}, J decreases in all systems as temperature rises from 280 K to 320 K (Fig. 5d – f), but the magnitude of this suppression varies markedly between amine types. We first consider the CHO-amine systems (NH_2CHO and CH_3NHCHO). Over the 280 – 320 K range, their J values decrease by approximately 1 order of magnitude (Fig. 5e), and they remain within the same order of magnitude as those of their parent amine systems across the entire temperature range (Fig. 5f). This relatively modest thermal sensitivity indicates that CHO-amine-mediated nucleation can persist under both warm and cold atmospheric conditions. A possible explanation is that, although CHO-amine clusters possess weaker binding energies and are therefore easier to thermal dissociation, their nucleation pathways apparently compensate through alternative routes, keeping J from dropping sharply. We now turn to the saturated OH-amine systems (NH_2OH and CH_3NHOH). These exhibit extreme thermal sensitivity (Fig. 5d): their J values decrease by 1 – 5 orders of magnitude over the same temperature range, and at elevated temperatures they fall 3 – 14 orders of magnitude below those of their corresponding parent amine systems (Fig. 5f). This pronounced drop likely arises from the stronger hydrogen-bonding

https://doi.org/10.5194/egusphere-2026-4704
Preprint. Discussion started: 24 August 2026

networks formed by OH-amines. While these networks are thermodynamically favorable at low temperatures, they become rapidly destabilized by thermal agitation as temperature rises, leading to a steep decline in formation rates.

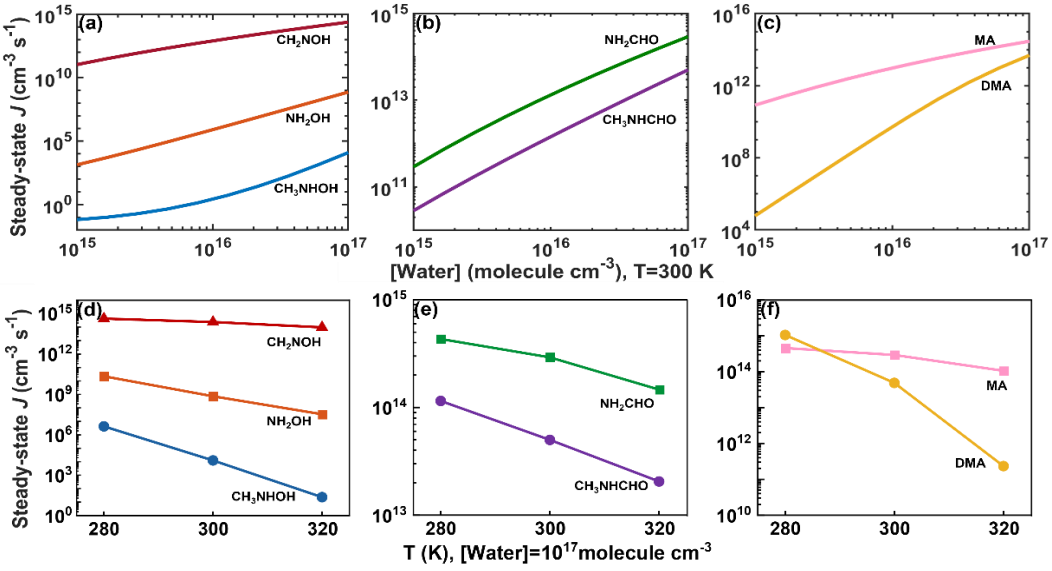

Figure 5 Formation rates (*J*) of critical clusters from ACDC simulations. (a)–(c) *J* as a function of [H_2O] at 300 K; (d)–(f) *J* as a function of temperature at [H_2O] = 10^{17} molecules cm^{-3}. (a,d) OH-amine systems; (b,e) CHO-amine systems; (c,f) Parent amine systems.

3.4 Atmospheric implications

Several implications for atmospheric new particle formation emerge from the combined kinetic, thermodynamic, and nucleation simulations presented above. With respect to the initial sulfate formation step, the hydrolysis rate constants (k_p) range from 10^{16} to 10^{26} s^{-1} for OH-amines and from 10^{16} to 10^{19} s^{-1} for CHO-amines. These values far exceed the •OH-oxidation sink of 1.3×10^6 s^{-1}. This confirms that the sulfate formation pathway can effectively compete with the conventional •OH-oxidation route. Growth pathway analysis further reveals that NH_2OH and CH_2NOH possess flexible multi-core routes that accelerate cluster growth toward critical sizes. In contrast, CH_3NHOH and CHO-amines are largely confined to single- or double-core pathways. Beyond the sulfate formation and growth pathway levels, simulations of cluster formation rates (J) reveal functional equivalence between certain ozonation products and their parent amines. CH_2NOH and NH_2CHO achieve J values of $10^{11} – 10^{14}$ cm^{-3} s^{-1}, comparable to that of methylamine. CH_3NHCHO reaches 5.00×10^{13} cm^{-3} s^{-1} under high humidity, close to the dimethylamine system at ~10^{13} cm^{-3} s^{-1}. This implies that ozonation does not terminate amine-driven nucleation. Rather, the products sustain particle formation downwind of emission sources, effectively extending the spatial footprint of amine emissions on aerosol populations.

The strong humidity dependence also indicates that this mechanism operates most effectively in moist environments, such as marine boundary layers, tropical regions, and cloud or fog processing conditions. In these settings, abundant water clusters promote both the initial sulfate formation and subsequent cluster growth toward critical sizes. For CHO-amines especially,

https://doi.org/10.5194/egusphere-2026-4704
Preprint. Discussion started: 24 August 2026

their formation rates reach 10^{13} – 10^{14} cm^{-3} s^{-1} only above RH ≈ 80%, confirming that high humidity is an essential prerequisite for their nucleation activity. Temperature further defines the relevance of individual species. Saturated OH-amines exhibit extreme thermal sensitivity. Their formation rates drop by 3 – 14 orders of magnitude from 280 to 320 K, confining their contribution primarily to cold climates or seasons. CHO-amines, by contrast, decrease by only about one order of magnitude over the same temperature range. They remain comparable to their parent amines across a broad thermal range, making them more competitive under warm conditions. Humidity and temperature together shape distinct environmental preferences for different ozonation products. OH-amine-mediated pathways may be feasible in polar regions and wintertime, while CHO-amine-mediated ones become more relevant in the tropics and summer months.

The above distinct cluster growth behaviors among amine derivatives preclude simplified lumped parameterization in aerosol models. For example, CH_3NHOH lacks the multi-core flexibility of NH_2OH and CH_2NOH and follows exclusively a single-core addition route. Apart from differences in cluster growth pathways, species-specific humidity and temperature sensitivities will create substantial biases in simulated NPF rates. To mitigate these biases, future aerosol modeling efforts should implement species-specific parameterization for amine ozonation byproducts rather than uniform lumped parameters, to capture their divergent cluster growth and meteorological responses. Continuous field measurements of ambient OH- and CHO-amines are also needed to better constrain model simulations of regional NPF and relevant impacts.

4 Conclusions

In this work, we combine quantum chemical calculations and cluster dynamics simulations to quantitatively evaluate the nucleation activity of five amine ozonation products. Our results show that OH-amines lower the SO_2 hydrolysis barrier to 2.57 – 19.42 kcal/mol, shifting the rate-limiting step to ozonation (17.20 – 24.25 kcal/mol), while CHO-amines require $(H_2O)_3$ clusters to bring the hydrolysis barrier down to 9.51 – 11.51 kcal/mol, making the overall process kinetically accessible. The apparent pseudo-first-order rate constants for hydrolysis range from 10^{24} to 10^{26} s^{-1} for OH-amines and 10^{16} to 10^{19} s^{-1} for CHO-amines, exceeding the •OH oxidation sink (1.3×10^6 s^{-1}) by orders of magnitude, which underscores the dominance of this non-radical pathway under haze conditions. In terms of cluster growth, NH_2OH and CH_2NOH allow multi-core cooperative routes, whereas CH_3NHOH and both CHO-amines are restricted to fewer pathways, highlighting structural effects on growth flexibility. Humidity universally enhances cluster formation, with J increasing by 3–6 orders of magnitude as water concentration rises from 10^{15} to 10^{17} cm^{-3}. Temperature sensitivity, however, is strongly species-dependent: for NH_2OH and CH_3NHOH, J falls by 3 – 14 orders of magnitude between 280 and 320 K, whereas CHO-amines drop by only about one order over the same interval. Notably, the J values of CH_2NOH and NH_2CHO (10^{11} – 10^{14} cm^{-3} s^{-1}) match those of methylamine, and CH_3NHCHO reaches 5.00×10^{13} cm^{-3} s^{-1} at high humidity, comparable to dimethylamine (~10^{13} cm^{-3} s^{-1}), confirming that ozonation products sustain NPF rather than terminating it. These findings, together with the species-specific responses to temperature and humidity, call for explicit treatment of amine oxidation products in aerosol models, rather than lumped parameterization, and for targeted field observations to constrain their regional NPF impacts.

https://doi.org/10.5194/egusphere-2026-4704
Preprint. Discussion started: 24 August 2026

Author contributions. WZ and TA designed the research goals, aims and methodology. JL and RL contributed to calculations and data processing. WZ analysed the data and wrote the manuscript. WZ, JL, YZ, RL, SZ, GL, YJ and TA proofread and commented on the paper.

Supplement. The supplement related to this article is available online at:

Competing interests. The authors declare that they have no conflict of interest.

Disclaimer. Publisher's note: Copernicus Publications remains neutral with regard to jurisdictional claims made in the text, published maps, institutional affiliations, or any other geographical representation in this paper. While Copernicus Publications makes every effort to include appropriate place names, the final responsibility lies with the authors.

Financial support. This work is supported by the NSFC (22522602 and 42277081), the Basic and Applied Basic Research Fund Project of Guangdong Province (2024A1515012691), the Guangzhou Science and Technology Program (2025A04J5188), and the Introduction Innovative and Research Teams Project of Guangdong Pearl River Talents Program (2023ZT10L102).

Review statement.

References

Almeida, J., Schobesberger, S., Kurten, A., Ortega, I. K., Kupiainen-Maatta, O., Praplan, A. P., Adamov, A., Amorim, A., Bianchi, F., Breitenlechner, M., David, A., Dommen, J., Donahue, N. M., Downard, A., Dunne, E., Duplissy, J., Ehrhart, S., Flagan, R. C., Franchin, A., Guida, R., Hakala, J., Hansel, A., Heinritzi, M., Henschel, H., Jokinen, T., Junninen, H., Kajos, M., Kangasluoma, J., Keskinen, H., Kupc, A., Kurten, T., Kvashin, A. N., Laaksonen, A., Lehtipalo, K., Leiminger, M., Leppa, J., Loukonen, V., Makhmutov, V., Mathot, S., McGrath, M. J., Nieminen, T., Olenius, T., Onnela, A., Petaja, T., Riccobono, F., Riipinen, I., Rissanen, M., Rondo, L., Ruuskanen, T., Santos, F. D., Sarnela, N., Schallhart, S., Schnitzhofer, R., Seinfeld, J. H., Simon, M., Sipila, M., Stozhkov, Y., Stratmann, F., Tome, A., Trostl, J., Tsagkogeorgas, G., Vaattovaara, P., Viisanen, Y., Virtanen, A., Vrtala, A., Wagner, P. E., Weingartner, E., Wex, H., Williamson, C., Wimmer, D., Ye, P., Yli-Juuti, T., Carslaw, K. S., Kulmala, M., Curtius, J., Baltensperger, U., Worsnop, D. R., Vehkamaki, H., and Kirkby, J.: Molecular understanding of sulphuric acid-amine particle nucleation in the atmosphere, Nature, 502, 359-363, 10.1038/nature12663, 2013.

Anglada, J. M., Hoffman, G. J., Slipchenko, L. V., Costa, M. M., Ruiz-Lopez, M. F., and Francisco, J. S.: Atmospheric significance of water clusters and ozone-water complexes, J. Phys. Chem. A, 117, 10381-10396, 10.1021/jp407282c, 2013.

Bai, X., Lian, Y., Peng, J., Mao, H., and Jiang, S.: Ethylenediamine-enhanced iodic acid nucleation: Mechanistic insights into marine new particle formation, Environ. Sci. Technol., 59, 22772-22783, 10.1021/acs.est.5c08562, 2025.

Brean, J., Rowell, A., Beddows, D. C. S., Shi, Z., and Harrison, R. M.: Estimates of future new particle formation under different emission scenarios in Beijing, Environ. Sci. Technol., 57, 4741-4750, 10.1021/acs.est.2c08348, 2023.

Brean, J., Rowell, A., Beddows, D. C. S., Weinhold, K., Mettke, P., Merkel, M., Tuch, T., Rissanen, M., Maso, M. D., Kumar, A., Barua, S., Iyer, S., Karppinen, A., Wiedensohler, A., Shi, Z., and Harrison, R. M.: Road traffic emissions lead to much enhanced new particle formation through increased growth rates, Environ. Sci. Technol., 58, 10664-10674, 10.1021/acs.est.3c10526, 2024.

https://doi.org/10.5194/egusphere-2026-4704
Preprint. Discussion started: 24 August 2026

Cai, S., Liu, T., Huang, X., Song, Y., Wang, T., Sun, Z., Gao, J., and Ding, A.: Important role of low cloud and fog in sulfate aerosol formation during winter haze over the North China Plain, Geophys. Res. Lett., 51, e2023GL106597, 10.1029/2023gl106597, 2024.

Canneaux, S., Bohr, F., and Henon, E.: KiSThelP: A program to predict thermodynamic properties and rate constants from quantum chemistry results, J. Comput. Chem., 35, 82-93, https://doi.org/10.1002/jcc.23470, 2014.

Deng, C., Fu, Y., Dada, L., Yan, C., Cai, R., Yang, D., Zhou, Y., Yin, R., Lu, Y., Li, X., Qiao, X., Fan, X., Nie, W., Kontkanen, J., Kangasluoma, J., Chu, B., Ding, A., Kerminen, V.-M., Paasonen, P., Worsnop, D. R., Bianchi, F., Liu, Y., Zheng, J., Wang, L., Kulmala, M., and Jiang, J.: Seasonal characteristics of new particle formation and growth in urban Beijing, Environ. Sci. Technol., 54, 8547-8557, 10.1021/acs.est.0c00808, 2020.

Doye, J. P. K. and Wales, D. J.: Thermodynamics of global optimization, Phys. Rev. Lett., 80, 1357-1360, 10.1103/PhysRevLett.80.1357, 1998.

Fang, Y., Ye, C., Wang, J., Wu, Y., Hu, M., Lin, W., Xu, F., and Zhu, T.: Relative humidity and O_3 concentration as two prerequisites for sulfate formation, Atmos. Chem. Phys., 19, 12295-12307, 10.5194/acp-19-12295-2019, 2019.

Frisch, M. J., Trucks, G. W., Schlegel, H. B., Scuseria, G. E., Robb, M. A., Cheeseman, J. R., Scalmani, G., Barone, V., Petersson, G. A., Nakatsuji, H., Li, X., Caricato, M., Marenich, A. V., Bloino, J., Janesko, B. G., Gomperts, R., Mennucci, B., Hratchian, H. P., Ortiz, J. V., Izmaylov, A. F., Sonnenberg, J. L., Williams, Ding, F., Lipparini, F., Egidi, F., Goings, J., Peng, B., Petrone, A., Henderson, T., Ranasinghe, D., Zakrzewski, V. G., Gao, J., Rega, N., Zheng, G., Liang, W., Hada, M., Ehara, M., Toyota, K., Fukuda, R., Hasegawa, J., Ishida, M., Nakajima, T., Honda, Y., Kitao, O., Nakai, H., Vreven, T., Throssell, K., Montgomery Jr., J. A., Peralta, J. E., Ogliaro, F., Bearpark, M. J., Heyd, J. J., Brothers, E. N., Kudin, K. N., Staroverov, V. N., Keith, T. A., Kobayashi, R., Normand, J., Raghavachari, K., Rendell, A. P., Burant, J. C., Iyengar, S. S., Tomasi, J., Cossi, M., Millam, J. M., Klene, M., Adamo, C., Cammi, R., Ochterski, J. W., Martin, R. L., Morokuma, K., Farkas, O., Foresman, J. B., and Fox, D. J.: Gaussian 09 [code], 2009.

Fukui, K.: The path of chemical reactions - the IRC approach, Acc. Chem. Res., 14, 363-368, 10.1021/ar00072a001, 1981.

Ge, P., Luo, G., Huang, W., Xie, H., Chen, J., and Luo, Y.: Theoretical study of the hydration effects on alkylamine and alkanolamine clusters and the atmospheric implication, Chemosphere, 243, 125323, https://doi.org/10.1016/j.chemosphere.2019.125323, 2020.

Ge, Y., Liu, Y., Chu, B., He, H., Chen, T., Wang, S., Wei, W., and Cheng, S.: Ozonolysis of trimethylamine exchanged with typical ammonium salts in the particle phase, Environ. Sci. Technol., 50, 11076-11084, 10.1021/acs.est.6b04375, 2016.

He, G. and He, H.: Water promotes the oxidation of SO_2 by O_2 over carbonaceous aerosols, Environ. Sci. Technol., 54, 7070-7077, 10.1021/acs.est.0c00021, 2020.

Henschel, H., Kurtén, T., and Vehkamäki, H.: Computational study on the effect of hydration on new particle formation in the sulfuric acid/ammonia and sulfuric acid/dimethylamine systems, J. Phys. Chem. A, 120, 1886-1896, 10.1021/acs.jpca.5b11366, 2016.

Kirkpatrick, S., Gelatt, C. D., and Vecchi, M. P.: Optimization by simulated annealing, Science, 220, 671-680, 10.1126/science.220.4598.671, 1983.

Li, C., Chen, J., Xie, H. B., Zhao, Y., Xia, D., Xu, T., Li, X., and Qiao, X.: Effects of Atmospheric Water on .OH-initiated oxidation of organophosphate flame retardants: A DFT investigation on TCPP, Environ. Sci. Technol., 51, 5043-5051, 10.1021/acs.est.7b00347, 2017.

Li, X. and Bourg, I. C.: Phase state, surface tension, water activity, and accommodation coefficient of water-organic clusters near the critical size for atmospheric new particle formation, Environ. Sci. Technol., 57, 13092-13103, 10.1021/acs.est.2c09627, 2023.

Liu, J., Fang, S., Liu, W., Wang, M., Tao, F.-M., and Liu, J.-y.: Mechanism of the gaseous hydrolysis reaction of SO_2: Effects of NH_3 versus H_2O, J. Phys. Chem. A, 119, 102-111, 10.1021/jp5086075, 2015.

Liu, Y., Xie, H. B., Ma, F., Chen, J., and Elm, J.: Amine-enhanced methanesulfonic acid-driven nucleation: Predictive model and cluster formation mechanism, Environ. Sci. Technol., 56, 7751-7760, 10.1021/acs.est.2c01639, 2022.

Long, B., Bao, J. L., and Truhlar, D. G.: Reaction of SO_2 with OH in the atmosphere, Phys. Chem. Chem. Phys., 19, 8091-8100, 10.1039/C7CP00497D, 2017.

Loukonen, V., Kurtén, T., Ortega, I. K., Vehkamäki, H., Pádua, A. A. H., Sellegri, K., and Kulmala, M.: Enhancing effect of dimethylamine in sulfuric acid nucleation in the presence of water – a computational study, Atmos. Chem. Phys., 10, 4961-4974, 10.5194/acp-10-4961-2010, 2010.

https://doi.org/10.5194/egusphere-2026-4704
Preprint. Discussion started: 24 August 2026

Lv, G., Nadykto, A. B., Sun, X., Zhang, C., and Xu, Y.: Towards understanding the role of amines in the SO_2 hydration and the contribution of the hydrated product to new particle formation in the Earth's atmosphere, Chemosphere, 205, 275-285, 10.1016/j.chemosphere.2018.04.117, 2018.

McGrath, M. J., Olenius, T., Ortega, I. K., Loukonen, V., Paasonen, P., Kurtén, T., Kulmala, M., and Vehkamäki, H.: Atmospheric Cluster Dynamics Code: a flexible method for solution of the birth-death equations, Atmos. Chem. Phys., 12, 2345-2355, 10.5194/acp-12-2345-2012, 2012.

Shen, Q., Liu, Y. D., and Zhong, R.: Degradation mechanisms of simple aliphatic amines under ozonation: a DFT study, Environ. Sci.: Processes Impacts, 23, 480-490, 10.1039/D0EM00476F, 2021.

Stewart, J. J. P.: Optimization of parameters for semiempirical methods V: Modification of NDDO approximations and application to 70 elements, J. Mol. Model., 13, 1173-1213, 10.1007/s00894-007-0233-4, 2007.

Vereecken, L. and Francisco, J. S.: Theoretical studies of atmospheric reaction mechanisms in the troposphere, Chem. Soc. Rev., 41, 6259-6293, 10.1039/C2CS35070J, 2012.

Wang, S., Zeng, X. C., Li, H., and Francisco, J. S.: A possible unaccounted source of atmospheric sulfate formation: amine-promoted hydrolysis and non-radical oxidation of sulfur dioxide, Chem. Sci., 11, 2093-2102, 10.1039/C9SC04756E, 2020.

Wine, P. H., Thompson, R. J., Ravishankara, A. R., Semmes, D. H., Gump, C. A., Torabi, A., and Nicovich, J. M.: Kinetics of the reaction OH + SO_2 + M .fwdarw. $HOSO_2$ + M. Temperature and pressure dependence in the fall-off region, J. Phys. Chem., 88, 2095-2104, 10.1021/j150654a031, 1984.

Xiong, H., Liu, X., Sun, C., Zhang, X., Wang, X., Lin, J., Xue, L., Sun, X., Shang, X., Ma, F., Xie, H., Chen, J., Yan, G., Shu, J., Fu, H., Wang, L., Rudich, Y., George, C., Mellouki, A., Zhao, D., Wang, X., Herrmann, H., and Chen, J.: Atmospheric water cluster–catalyzed formation of nitroaromatics as a secondary aerosol source, Sci. Adv., 11, eadv7805, doi:10.1126/sciadv.adv7805, 2025.

Yao, L., Garmash, O., Bianchi, F., Zheng, J., Yan, C., Kontkanen, J., Junninen, H., Mazon, S. B., Ehn, M., Paasonen, P., Sipilä, M., Wang, M., Wang, X., Xiao, S., Chen, H., Lu, Y., Zhang, B., Wang, D., Fu, Q., Geng, F., Li, L., Wang, H., Qiao, L., Yang, X., Chen, J., Kerminen, V.-M., Petäjä, T., Worsnop, D. R., Kulmala, M., and Wang, L.: Atmospheric new particle formation from sulfuric acid and amines in a Chinese megacity, Science, 361, 278-281, 10.1126/science.aao4839, 2018.

Zhang, J. and Dolg, M.: ABCluster: the artificial bee colony algorithm for cluster global optimization, Phys. Chem. Chem. Phys., 17, 24173-24181, 10.1039/C5CP04060D, 2015.

Zhang, W., Zheng, D., Lao, J., Li, R., Chen, B., Chen, J., Zhong, J., Ji, Y., Li, G., Francisco, J. S., and An, T.: Sulfate promotes amine salt ozonation in atmospheric aerosols, J. Am. Chem. Soc., 147, 34327-34338, 10.1021/jacs.5c04343, 2025.